Zero-dispersion waveguide of sub-skin-depth terahertz plasmons using metallic nanowires

Jie Yang (杨 洁)*, Yueping Niu (钮月萍), Gongwei Lin (林功伟), Yihong Qi (祁义红), and Shangqing Gong (龚尚庆)**

Department of Physics, East China University of Science and Technology, Shanghai 200237, China

**Corresponding author: yangjie7898@ecust.edu.cn; **corresponding author: sqgong@ecust.edu.cn*

Received April 9, 2013; accepted May 20, 2013; posted online August 2, 2013

Global change in the dispersive behavior of terahertz (THz) plasmons on metal wires with wide radii ranging from 5 nm to 0.5 mm is systematically investigated. Through rigorous numerical calculations, we find that the dispersion of a metal wire with a radius of 5 nm increases by about 4-6 orders of magnitude compared with the case of a metallic wire with a radius of 0.5 mm. Zero-dispersion points appear when the frequency is lower than 3 THz, and the positions of the zero-dispersion points can shift with the frequency. Finally, we provide an explicit expression that agrees very well with the numerical calculations.

OCIS codes: 240.6680, 260.3090, 230.7370, 260.3910.

doi: 10.3788/COL201311.082401.

Terahertz (THz) radiation, which lies in the frequency gap between infrared and microwaves, is typically described as electromagnetic waves with frequencies ranging from 0.1 to 10 THz (or from 30 μm to 3 mm in wavelength). Given the rapid development of laser technology, various techniques for the generation and detection of THz radiation have been proposed. These techniques have helped promote the application of THz technology in many aspects, such as sensing, imaging, communications, and spectroscopy[1−3]. However, conventional metal waveguides for microwave radiation and dielectric fibers for visible radiation cannot be used in THz waveguides because of high losses in this spectral range. Furthermore, the extensive use of broadband pulses in the THz regime imposes a strict constraint of low dispersion, which is a significant obstacle to the development of effective THz waveguides. In 2004, Wang *et al*. demonstrated that a single metal wire with a diameter about 1 mm could be used as a THz waveguide with low propagation loss and dispersion[4]. Since then, many interesting theoretical and experimental works on metal wire THz waveguides have been carried out[5−19]. THz waveguide effects on metal wire originate from azimuthally polarized surface plasmon polaritons (SPPs)[5]. SPPs, which propagate on metal-dielectric interfaces, decay exponentially in metal and dielectric medium. The skin-depth of electromagnetic waves in metal is determined by the penetration distance at which the electric field falls to 1/e, and the value of skin-depth is defined as $\delta = \lambda_0/[2\pi \mathrm{Im}(\varepsilon_m^{[1/2]})]$[20]. For SPPs in the THz wavelength range and other low frequency radiation forms, skin-depth is a very important length scale, which is at the submicrometre level throughout the THz spectral range. Wang and Mittleman studied the dispersive behavior of SPPs on metal wires with a minimum radius of several microns[10]. However to date few papers discussing the dispersive behavior of sub-skin-depth THz plasmons on metallic nanowires have been published.

In this letter, we propose a sub-skin-depth THz waveguide with negligible loss and zero-dispersion. Our findings can guide future designs of THz waveguides with relatively small radii to achieve zero group-velocity dispersion. Although small values of dispersion and loss can be obtained by increasing the metal wire radius, this approach not only significantly increases the costs of the resulting waveguide, but is also disadvantageous to the integration of systems. Furthermore, impulses are easily broadened and cannot meet requirements for high fidelity in modern communications even when the values of dispersion are small. Using zero-dispersion values for communications is common in other communication systems. For example, in fiber communications, wavelengths of 1 310 and 1 550 nm are also considered zero-dispersion wavelengths[21].

We study the dispersion of the THz plasmon of metallic wires with wide radii ranging from 5 nm to 0.5 mm. The numerical calculations are based on a rigorous deduction of Maxwell's equation. The results reveal that the dispersion of a metal wire with a radius of 5 nm can increase by about 4-6 orders of magnitude when the frequency is located in the THz radiation range compared with a metallic wire with a radius of 0.5 nm. We also shown that very small fluctuations appear as the dispersion changes at lower frequencies and discuss several principles of the positions of the fluctuations. We illustrate that zero-dispersion points exist during fluctuation. Finally, we discuss an explicit expression for the dispersion behavior that agrees well with the numerical calculations. These findings may help guide future designs of THz waveguides with relatively small radii to achieve zero group-velocity dispersion and negligible loss, which saves costs, contributes to the integration of the system, and ensures the high fidelity of modern communications.

Considering a cylindrical metal wire surrounded by air. We are interested in an axially symmetric eigenmode, where the relations $\partial \mathrm{E}/\partial\varphi{=}0$ and $\partial \mathrm{H}/\partial\varphi{=}0$ always hold. For transverse magnetic (TM) polarization of a nonmagnetic metal, substitution of the above mentioned relations into Maxwell's equations[22] and use of the continuities of E_z and H_φ at the interface can yield the following eigen-

equation[5,12,13,15,23,24]:

$$\frac{\varepsilon_m}{\kappa_m}\frac{I_1(k_0\kappa_m R)}{I_0(k_0\kappa_m R)}+\frac{1}{\kappa_a}\frac{K_1(k_0\kappa_a R)}{K_0(k_0\kappa_a R)}=0, \quad (1)$$

where $\kappa_a=[(n_{\rm eff})^2-1]^{1/2}$, $\kappa_m=[(n_{\rm eff})^2-\varepsilon_m]^{1/2}$, and $n_{\rm eff}$ is the effective index of the eigenmode. $n_{\rm eff}$ is a very important parameter for the propagation properties of the eigenmode. The real and imaginary parts of the term represent the dispersion and loss of the eigenmode, respectively. The definition of $n_{\rm eff}$ can be expressed as $n_{\rm eff}=k/k_0$, where k and k_0 denote the wave numbers of the eigenmode in the surface plasmon and in free space, respectively. ε_m is the relative permittivity of the metal. $I_0(.)$, $K_0(.)$, $I_1(.)$, and $K_1(.)$ are modified Bessel functions. $k_0=2\pi/\lambda_0$, where λ_0 is the wavelength in free space, and R is the radius of the metal wire.

We use rigorous numerical calculations to obtain the exact values of the dispersion of metal wires with wide radii ranging from 5 nm to 0.5 mm. Copper metal wires are chosen, and the frequency is set to 5 THz. The corresponding ε_m value is $\varepsilon_m=-1.0\times10^5+{\rm j}4.7\times10^4$ according to a fitted Drude formula for copper[25]. The values of dispersion are obtained according to the rigorous definition of the dispersion, which can be written as

$$D=\frac{\rm d}{{\rm d}\lambda}[{\rm Re}(n_{\rm eff})], \quad (2)$$

where λ denotes the wavelength of the eigenmode of the propagating surface plasmon. The calculation results are shown in Fig. 1. We can see that the absolute values of dispersion for metal wires with radii of 5 nm and 0.5 mm are about 2 and 2.0×10^{-4}, respectively, so the former is about 4 orders of magnitude larger than the later. The ends of the chosen range of metal wire radii are 5 nm and 0.5 mm; that is to say, one of the ends is smaller than skin-depth, where the value of skin-depth δ is 28.5 nm according to the definition of $\delta=\lambda_0/[2\pi{\rm Im}(\varepsilon_m{}^{1/2})]$, and the other is far larger than skin-depth. We can only obtain the absolute values of dispersions because only positive values can be scaled by logarithm for wide regions of radius and dispersion, as shown in Fig. 1. For unity, in Figs. 2 and 5 we also use absolute values of dispersion, which are the values of concern in this work.

To observe the dispersion behavior of the metal wire at lower frequencies of THz radiation, we choose 0.5 THz as

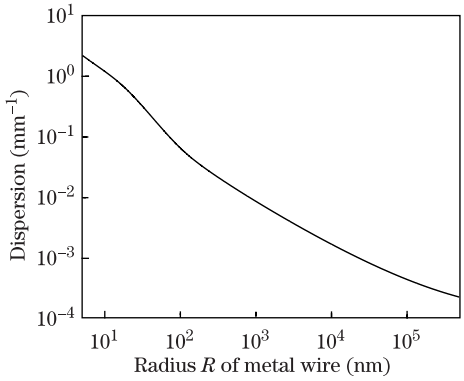

Fig. 1. Changes in the values of dispersion in the wide region of a copper wire with a radius ranging from 5 nm to 0.5 mm at 5 THz.

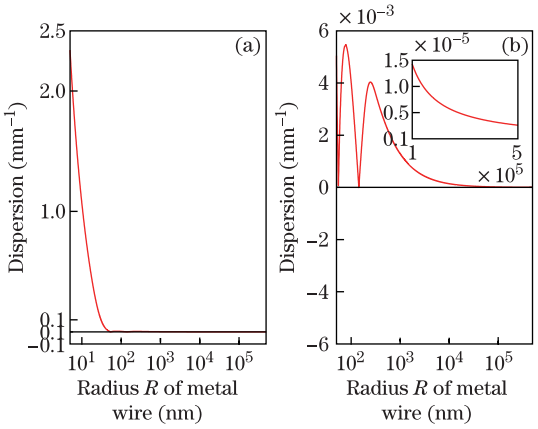

Fig. 2. Dispersions in the wide region of copper wires with radii ranging from 5 nm to 0.5 mm at 0.5 THz. (a) Global image of the changes in dispersion of copper wires with radii ranging from 5 nm to 0.5 mm at 0.5 THz. (b) Enlarged image of the changes in dispersion of copper wires with radii ranging from 50 nm to 0.5 mm. Inset: Enlarged image of the dispersion of copper wires with radii ranging from 0.1 mm to 0.5 mm.

an example, as shown in Fig. 2. All other parameters are identical to those in Fig. 1 except for the frequency. The corresponding ε_m value is $\varepsilon_m=-6.3\times10^5+{\rm j}2.77\times10^6$ according to a fitted Drude formula for copper[25]. In Fig. 2(a), we show a global image of the changes in dispersion and find that the dispersion in a metal wire with a radius of 5 nm at 0.5 THz is about 2.3. Some fluctuations may be observed when the radius of the metal wire is larger than 50 nm. Fig. 2(b) and the inset of Fig. 2(b) show enlarged images of the changes in dispersion of wires with radii ranging from 50 nm to 0.5 mm and 0.1 mm to 0.5 mm respectively. The dispersion of the metal wire with a radius of 0.5 mm is about 2×10^{-6}. Compared with the case of the wire of 5 nm in Fig. 2(a), the dispersion of the metal wire with a radius of 5 nm is about 6 orders of magnitude higher. Thus, the increment of dispersion values of metal wires at 0.5 THz is larger than that of metal wires at 5 THz.

Although the values of dispersion increase rapidly with the decrease in radius of the metal wire, zero-dispersion points may be observed when the radii of metal wires are about 55 and 140 nm, as shown in Fig. 2(b). The appearance of zero-dispersion points is a very useful property for long-distance transmission in THz communication technology, and it can help us design THz waveguides with relatively small radii to achieve zero-dispersion points.

Two parameters that determine the effectiveness of the waveguide are loss and dispersion. In the following discussion, we study the losses at the zero-dispersion points. To describe the zero-dispersion points shown in Fig. 2, we calculate the exact values of the attenuation coefficients of the wires with radii ranging from 50 to 150 nm, which are shown in Fig. 3. The attenuation coefficient α is related to the imaginary part of the effective index by the relation $\alpha=k_0Im(n_{\rm eff})$. From Fig. 3, we can see that the loss in the wire of radius 55 nm is about 1.2 mm^{-1}, and that the loss in the wire of radius 140 nm is about 0.25 mm^{-1}. Losses at the zero-dispersion points initially seem to be far larger in metal wires with small radii than in metal wire waveguide with

large radii. For example, the loss in the metal wire with a radius of 0.9 mm is only about 0.03 cm^{-1}[26]. However, we consider the factual experimental fabrications of metallic nanowires. To the best of our knowledge, the lengths of metallic nanowires usually range from tens of nanometers to tens of microns[27−30]. Taking the larger attenuation coefficient α as an example, the amplitude of the propagation distance 100 μm for a copper wire with a radius of 55 nm is about $0.9E_0$ according to the relation of $E(x) = E_0 e^{-\alpha x}$, where E_0 represents the initial amplitude. The above loss is still an acceptable value of loss for the THz waveguide[26].

We now study the dispersion behavior of copper wires over the entire THz wave region. For comparison, we select parameters identical to those used above except for the frequency. Through rigorous numerical calculation, we conclude three main characteristics. Firstly, the trend of dispersion behavior is similar to those shown in Fig. 1 or 2 depending on the frequency. Specifically, when the frequency is lower than 3 THz, the change in dispersion is similar to that shown in Fig. 2; when the frequency is higher than 3 THz, the dispersion monotonically decreases with increasing radius, as shown in Fig. 1. Secondly, for two metal wires with radii of 5 nm and 0.5 mm, the increment of dispersion at low frequency is larger than that at high frequency. Thirdly, we note that the positions of zero-dispersion points change with the frequency and that the locations of zero-dispersion points as well as corresponding fluctuations shift toward smaller radii as the frequency increases and toward large radii as the frequency decreases. To describe our findings more clearly, a comparison of frequencies of 0.1, 0.4, and 2.5 THz is performed, and corresponding results are shown in Fig. 4. We use dispersion values instead of absolute values of dispersion in Fig. 4 to observe fluctuation shifts more clearly. The signs of the dispersion values in Fig. 4 change because the values of $\mathrm{Re}(n_{\mathrm{eff}})$ first decrease firstly and then increase with the wavelength.

We test the applicability of the properties described above in other nonmagnetic metals mentioned in Ref. [25]. We find that these properties perform well for all other nonmagnetic metals of Al, Ag, Au, Mo, W, Pd, Ti, Pb, Pt, and V, although slight differences in the specific values of increments and positions of zero-dispersion points may be observed.

We derive an approximate expression for the dispersion behavior. To obtain an explicit expression

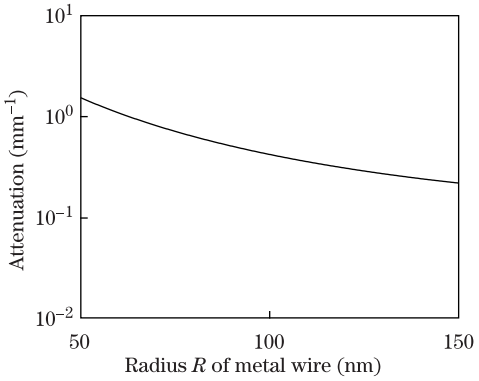

Fig. 3. Calculated values of attenuation coefficient for metal copper wires with radii ranging from 50 to 150 nm at 0.5 THz.

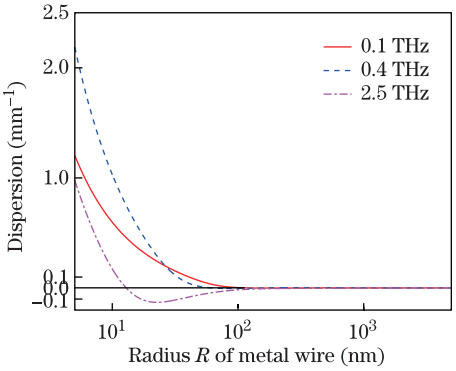

Fig. 4. Locations of zero-dispersion points at different frequencies.

that may accurately describe the dispersion, we first obtain an approximate formula for the effective index n_{eff}, which is hidden in Eq. (1) and cannot be solved analytically. Using the property $|{n_{\mathrm{eff}}}^2| << |\varepsilon_m|$ yields $\kappa_m \approx (-\varepsilon_m)^{1/2}$. The relation $K_1(k_0\kappa_a R) \approx (k_0\kappa_a R)^{-1}$ holds true for small R. Substituting these two approximations into Eq. (1), an approximate solution $\kappa_{a,3}$ for κ_a may be obtained

$$\kappa_{a,3} = \sqrt{\frac{a}{K_0(k_0 R \kappa_{a,2})}}, \tag{3}$$

where $\kappa_{a,2}$ and a are given by[15]

$$\kappa_{a,2} = \sqrt{a}\left[K_0\left(k_0 R\sqrt{\frac{a}{K_0(k_0 R\sqrt{a}\,)}}\right)\right]^{-1/2}, \tag{4}$$

$$a = \frac{1}{k_0 R\sqrt{-\varepsilon_m}}\frac{I_0(k_0 R\sqrt{-\varepsilon_m})}{I_1(k_0 R\sqrt{-\varepsilon_m})}. \tag{5}$$

The approximate value of $n_{\mathrm{eff},3}$ can be obtained from the relation

$$n_{\mathrm{eff},3} = \sqrt{\kappa_{a,3}^2 + 1}. \tag{6}$$

By substituting Eq.(6) into Eq.(2), we finally obtain an approximate expression D_a for the dispersion behavior as follows

$$D_a = \frac{1}{2n_{\mathrm{eff},3}}\frac{\mathrm{d}({\kappa_{a,3}}^2)}{\mathrm{d}\lambda}. \tag{7}$$

This approximate expression Eq. (7) can help us to determine values of dispersions without solving Eq. (1). To obtain a clear impression of the capability of Eq. (7), we calculate approximate Da and exact De values if dispersion with radii ranging from 5 nm to 0.5 mm. Copper metal wire is selected, and the frequency set to 0.5 THz (i.e., $\lambda = 0.6$ mm). The corresponding ε_m value is $\varepsilon_m = -6.3\times10^5 + \mathrm{j}2.77\times10^6$ according to a fitted Drude formula for copper[25]. Comparison results are shown in Fig. 5. The approximate values of D_a are in good agreement with the exact values of D_e over the considered radius range.

Finally, we test the applicability of the approximate formula for D_a in other nonmagnetic metals mentioned in Ref. [25] over the entire THz radiation range. The approximate formula Da performs well for all other nonmagnetic metals of Al, Ag, Au, Mo, W, Pd, Ti, Pb, Pt, and V.

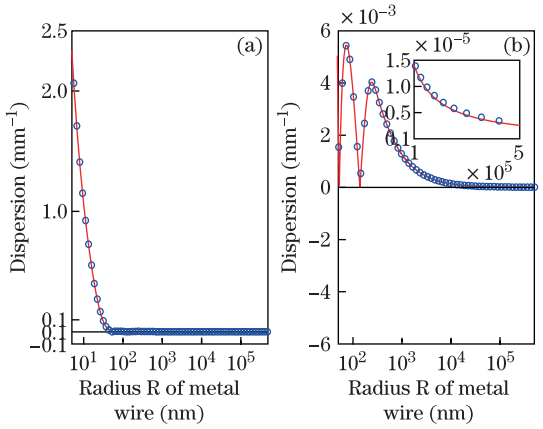

Fig. 5. (Color online) Comparison of the calculated absolute values of dispersion Da and the exact absolute values De for metal copper wire at 0.5 THz. The red solid curve is D_e and the blue "o" shows D_a. (a) Global image of the changes in dispersion of copper wires with radii ranging from 5 nm to 0.5 mm at 0.5 THz. (b) Enlarged image of the changes in dispersion of the copper wires with radii ranging from 50 nm to 0.5 mm. The inset shows an enlarged image of the copper wire with radii ranging from 0.1 mm to 0.5 mm.

In conclusion, we systematically investigate the dispersion of the THz plasmons of metallic wires with radii ranging from 5 nm to 0.5 mm. The numerical calculations are based on a rigorous deduction of Maxwell's equation. The results reveal that the dispersion of a metal wire with a radius of 5 nm increases by about 4-6 orders of magnitude compared with the case of a metallic wire with a radius of 0.5 mm when the frequency is located in the THz radiation range. Very small fluctuations appear during changes in dispersion at lower frequencies. We also obtain three characteristics of the positions of the fluctuations and observe that zero-dispersion points during fluctuation. Losses of metallic nanowires with radius at the zero-dispersion points 140 nm; however, the factual loss remains within acceptable limits. We also provide an explicit expression for the dispersion behavior that agrees well with the numerical calculations.

The excitation, coupling, and detection of sub-skin-depth plasmons are also important for the application of zero-dispersion THz waveguides. Recent research has proposed several methods through which improvement of THz coupling may be achieved[31,32]. We hypothesize that these methods may also be valid for sub-skin-depth plasmons. Similar to Ref. [15], we suggest the use of a radially polarized beam as the input beam to increase the coupling efficiency because of the excellent match between such a beam and the polarization of THz plasmons of a matallic nanowire.

Over all, these findings can help in future designs of THz waveguides with relative small radii to achieve zero group-velocity dispersion rates and negligible losses, which can not only save costs and improve the integration of the system but also ensure the high fidelity of modern communications.

We thank Prof. Qing Cao for the many helpful discussions. This work was supported by the China Post-Doctoral Science Foundation (Nos. 2011M500739 and 2011M500068), the Fundamental Research Funds for the Central Universities (No. WM1214019), and the National Natural Science Foundation of China (Nos. 11274112, 11204080, and 11074263).

References

1. B. B. Hu and M. C. Nuss, Opt. Lett. **20,** 1716 (1995).
2. A.Nahata, A. S. Weling, and T. F. Heinz, Appl. Phys. Lett. **69,** 2321 (1996).
3. M. J. Fitch and R. Osiander, Johns Hopkins. APL. Technical. Digest. **25,** 348 (2004).
4. K. Wang and D. M. Mittleman, Nature **432,** 376 (2004).
5. Q. Cao and J. Jahns, Opt. Express **13,** 511 (2005).
6. M. Walther, M. R. Freeman, and F. A. Hegmann, Appl. Phys. Lett. **87,** 261107 (2005).
7. T.-I. Jeon, J.-Q. Zhang, and D. Grischkowsky, Appl. Phys. Lett. **86,** 161904 (2005).
8. H. Cao and A. Nahata, Opt. Express **13,** 7028 (2005).
9. M. Wächter, M. Nagel, and H. Kurz, Opt. Express **13,** 10815 (2005).
10. K. Wang and D. M. Mittleman, J. Opt. Soc. Am. B **22,** 2001 (2005)
11. Y. Ji, E. Lee, J. Jang, and T.-I. Jeon, Opt. Express **16,** 271 (2008).
12. J. Yang, Q. Cao, and C. Zhou, Opt. Express **17,** 20806 (2009).
13. J. Yang, Q. Cao, and C. Zhou, J. Opt. Soc. Am. A **27,** 1608 (2010).
14. H. Liang, S. Ruan, M. Zhang, and H. Su, Opt. Commun. **283,** 262 (2010).
15. J. Yang, Q. Cao, and C. Zhou, Opt. Express **18,** 18550 (2010).
16. M. A. Seo and H. R. Park, Nat. Photon. **3,** 152 (2009).
17. L. Martin-Moreno, Nat. Photon. **3,** 131 (2009).
18. Y. Zhang, A. Berrier, and J. Rivas, Chin. Opt. Lett. **9,** 110014 (2011).
19. K. Chen, X. Feng, and Y. Huang, Chin. Opt. Lett. **11,** 022401 (2013).
20. A. K. Azad and W. Zhang, Opt. Lett. **30,** 2945 (2005).
21. G. P. Agrawal, *Fiber-Optic Communication Systems,* 2nd ed. (Wiley, New York, 1997).
22. M. Born and E. Wolf, *Principles of Optics,* 5th ed. (Pergamon Press, Oxford, 1975).
23. M. I. Stockman, Phys. Rev. Lett. **93,** 137404 (2004).
24. U. Schröter and A. Dereux, Phys. Rev. B **64,** 125420 (2001).
25. M. A. Ordal, R. J. Bell, R. W. Alexander, L. L. Long, and M. R. Querry, Appl. Opt. **24,** 4493 (1985).
26. K. Wang and D. M. Mittleman, J. Opt. Soc. Am. B **22,** 2001 (2005)
27. H. Ditlbacher, A. Hohenau, D. Wagner, U. Kreibig, M. Rogers, F. Hofer, F. R. Aussenegg, and J. R. Krenn, Phys. Rev. Lett. **95,** 257403 (2005).
28. A. V. Akimov and A. Mukherjee, Nature **450,** 402 (2007).
29. Y. Fedutik, V. V. Temnov, O. Schöps, U. Woggon, and M. V. Artemyev, Phy. Rev. Lett. **99,** 136802 (2007).
30. S. M. Bergin, Y.-H. Chen, A. R. Rathmell, P. Charbonneau, Z.-Y. Li, and B. J. Wiley, Nanoscale **4,** 1996 (2012).
31. G. Li, Z. Jin, X. Xue, X. Lin, G. Ma, S. Hu, and N. Dai, Appl. Phys. Lett. **100,** 191115 (2012).
32. S.-H., K. E. S., Lee Y. B., Ji and T.-I., Jeon Opt. Express **18,** 1289 (2010).